

Influence of Thermal Barriers on Heat Flow in High Quality Chemical Vapor Deposited Diamond

J. Hartmann,^{1,*} M. Costello,² and M. Reichling^{1,†}

¹*Fachbereich Physik, Freie Universität Berlin, Arnimallee 14, 14195 Berlin, Germany*

²*Materials Technology, GEC Marconi, Caswell, Towcester, United Kingdom*

(Received 3 March 1997)

Thermal barriers in high quality chemical vapor deposited (CVD) diamond were investigated by photothermal microscopy. High resolution measurements confirm that the in-plane heat transport is strongly limited by the presence of thermal barriers. Thermal resistances in the range of 10^{-9} to 10^{-8} m²K/W located at grain boundaries are extracted from photothermal line scans. Recently published data on macroscopic one-dimensional thermal transport in CVD diamond are well explained by the microscopic measurements in connection with a simple one-dimensional heat flow model. [S0031-9007(97)04906-5]

PACS numbers: 66.70.+f

Diamond is the material with the highest room temperature thermal conductivity [1], more than four times higher than that of copper. Its likewise high electrical resistance makes diamond a promising material for heat spreaders in high-power electronic devices [2]. Because of its outstanding thermal and electrical characteristics, diamond heat spreaders can reduce thermal load and, therefore, increase computation velocity and the lifetime of electronic devices [3]. Chemical vapor deposition (CVD) technologies now offer polycrystalline diamond films with properties well suited for thermal management applications [4]. Several physical properties of such films come close to that of natural diamond, however, a major limitation of thermal properties of this artificial material is still its composition of columnar grains with sizes of some tens of micrometers [1], separated from each other by grain boundaries or microcracks that may act as effective thermal barriers for lateral heat flow [5]. Therefore, the microscopic investigation of thermal properties of CVD diamond films is of particular interest for understanding their thermal anisotropy [6] and is of practical use of the development of materials for heat spreaders.

A variety of methods with different spatial resolution have been used to investigate thermal transport in diamond [7]. So far photothermal reflectance microscopy [8,9] is the only technique to qualify for μm -resolved microscopy investigations addressing single diamond grains or grain boundaries.

CVD grown diamond possesses a columnar structure strongly affecting the in-plane thermal conductivity κ_{\parallel} much more than the perpendicular thermal conductivity κ_{\perp} leading to a strong anisotropy measured with nonlocal averaging methods [6,7]. Surprisingly, an analysis of these macroscopic measurements in terms of phonon scattering mechanisms reveals a negligible influence of bare grain boundaries on thermal conductivity, while point and extended defects yield a major contribution. Accounting for this result it was concluded [10] that

defects aggregated at grain boundaries or microcracks result in effective thermal barriers, but an experimental verification of this statement is still lacking.

In the present paper we investigate single thermal barriers and clarify their influence on overall thermal conductivity. Thermal resistance located at barriers is determined quantitatively and a one-dimensional model is used to relate macroscopic thermal conductivity of CVD diamond to microscopic transport data.

The investigated sample was deposited by a standard CVD microwave plasma procedure on a tungsten substrate. After deposition the diamond layer was removed from the substrate, cut into a free-standing tile of $10 \times 10 \times 0.6$ mm³ and polished on both sides. The high optical transparency as well as Raman characterization confirmed the superior quality of the material. The good thermal quality of this sample has been demonstrated in a previous publication [9] where we measured the thermal conductivity inside single grains and obtained values up to 2250 W/mK, which is as high as that of highest quality natural diamond of type IIa [1]. The photothermal apparatus and the details of surface preparation necessary for photothermal reflectance measurements described in Ref. [9] were also used for the present study devoted to the investigation of thermal barriers.

To identify grain boundaries at the sample surface a polarizing microscope was used. Figure 1 shows a typical section of the sample demonstrating the grain structure. A detailed analysis revealed a grain size ranging from 10 to 60 μm at the surface of the growth side with an average of 40 μm . The inset displays a typical region where thermal transport across a grain boundary was studied. Care was taken to select a boundary with rather large adjacent grains (some 10 μm in diameter). This precaution kept the influence of other boundaries on the photothermal results to an absolute minimum. For measuring thermal transport across the boundary we used a thermorefectance line-scan technique [11], i.e., we keep pump and probe beam, each

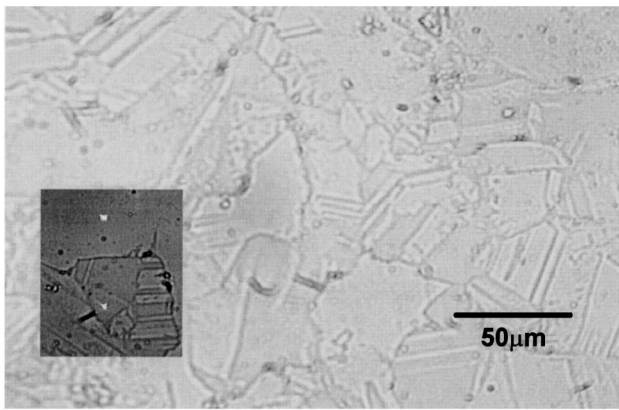


FIG. 1. Microscopy image of the CVD diamond surface demonstrating the surface grain structure. The inset shows one of the investigated thermal barriers on the same scale. The two bright spots are the foci of pump and probe beam, respectively, for large beam separation while the separation was $3 \mu\text{m}$ for photothermal measurements. The diameters of the laser spots are approximately $1.5 \mu\text{m}$.

of them focused to a spot of approximately $1.5 \mu\text{m}$ in diameter, at a fixed distance of $3 \mu\text{m}$ with respect to each other and scanned the sample on a line perpendicular to the boundary over a distance so that both beams crossed the thermal barrier. Amplitude and phase changes of the surface temperature modulation were recorded as a function of position. Typical scanning results obtained at 100 kHz modulation frequency are shown in Fig. 2. The strong influence of the boundary on the signal results in dramatic changes in the region where the beams are separated by the thermal boundary. Approaching the boundary closely with the pump beam, a gradual increase in signal amplitude is observed that results from thermal wave interference of the incoming and reflected thermal waves. The sharp decrease of signal amplitude [Fig. 2(a)] in the region where pump and probe beam are separated by the boundary is manifest to its thermal isolation and for a given modulation frequency its magnitude depends on the thermal resistance located at the thermal barrier and the thermal properties of the adjacent grains. A similar behavior can be found for the photothermal phase [Fig. 2(b)] where the phase lag in the boundary region accounts for the delay in thermal response across the boundary. As the thermal length for 100 kHz modulation frequency [9] is much larger than the beam separation the phase of incident and reflected heat current is nearly identical. Therefore, the interference effect can be seen only in the amplitude of the photothermal signal. The changes in amplitude and phase in this region provide a direct measure for the thermal resistance across the barrier and is quantified utilizing an analogy model of electrical and heat flow well established in literature [12].

Since there is no phase variation over the distance measured except in the vicinity of the grain boundary it is appropriate to assume one-dimensional heat flow from the

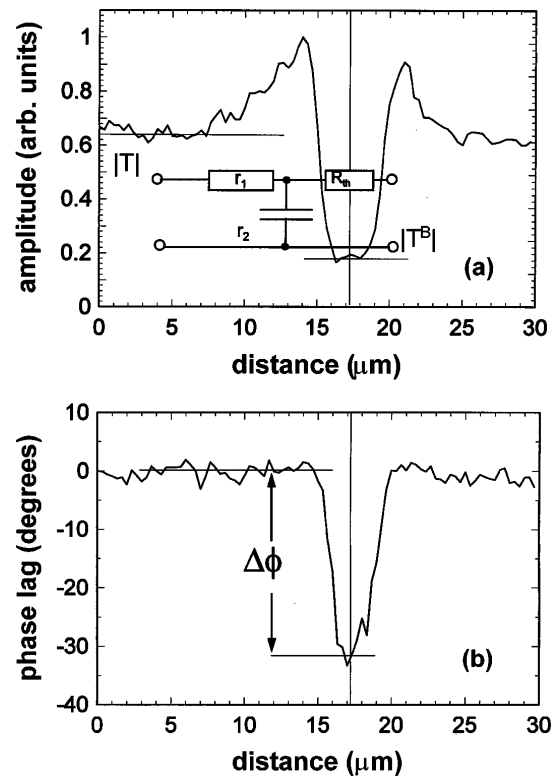


FIG. 2. Variation of amplitude (a) and phase (b) of the photothermal signal at 100 kHz modulation frequency when pump and probe beam (separated by $3 \mu\text{m}$ from each other) are scanned across a thermal barrier (vertical line). The inset is a schematic of the electric waveguide analog used for data analysis. A description of symbols is given in the text.

pump laser to the probe laser spot. The electrical waveguide analog to describe one-dimensional lateral heat flow is sketched in the inset of Fig. 2(a). Here $r_1 = 1/\kappa$ is the thermal series impedance per unit length corresponding to the thermal conductivity κ of the crystalline diamond between the two laser beams [13]. The shunt admittance $r_2 = i\omega\rho C_P$ represents the resistance due to the heat capacity ρC_P per unit length of the material at the modulation frequency ω . Both quantities together define the characteristic impedance of the grains adjacent to the barriers [13]. Because of the reflected thermal wave the heat flow across the barrier is reduced, which is taken into account by a real factor γ describing the amplitude enhancement in front of the barrier. Solving the equations for this linear network yields the following relation between temperature drop and thermal resistance R_{th} at the thermal barrier:

$$T^B/T = \gamma[1 - R_{\text{th}}(r_2/r_1)^{1/2}]. \quad (1)$$

The complex quantity T denotes the measured temperature with both beams far away from the thermal barriers; while T^B is the temperature with the thermal barrier between the two laser beams. The thermal resistance is most conveniently extracted from the phase drop $\Delta\phi$

that appears upon separation of the beams by the thermal barrier

$$R_{\text{th}} = \frac{\tan \Delta \phi}{\tan \Delta \phi - 1} (2/\omega \rho C_P \kappa)^{1/2}. \quad (2)$$

Applying this formula to a series of measurements on a number of grain boundaries yields thermal resistances ranging from 10^{-9} to 10^{-8} m² K/W with an average of 5×10^{-9} m² K/W when inserting bulk values for the diamond grain heat capacity and 2000 W/mK as an average thermal conductivity inside the grains [9]. The large range of thermal resistances is not due to experimental instability, but arises from the fact that there are grain boundaries with virtually no influence on lateral heat flow and others with a tremendous effect. The average value of the thermal resistance presented here has to be regarded as an overall average accounting for all the mentioned effects present in the sample under investigation and will be used as an effective value for further evaluation.

Next, we derive the macroscopically measured overall thermal conductivity $\kappa_{\text{av}}^{\text{1D}}$ of the CVD diamond sample for one-dimensional heat flow from parameters extracted from microscopic measurements, namely the thermal conductivity κ of the crystalline material inside the grains and the thermal resistance R_{th} located at barriers between grains. In case of one-dimensional heat flow, the polycrystalline sample can be regarded as a linear network of the thermal resistances of grains and resistances due to the thermal barriers [13]. To quantify the total thermal resistance of the polycrystalline sample we assume for simplicity a sample with length A having cubic grains with an average length a and, therefore, a total number of $(A/a - 1)$ grain boundaries within the sample. The total thermal resistance $R_{\text{th}}^{\text{1D}}$ for one-dimensional heat flow can then be described as the sum of the thermal resistance of the bulk material plus the additional resistances at all grain boundaries, and for the overall conductivity we find

$$\kappa_{\text{av}}^{\text{1D}} = A/R_{\text{th}}^{\text{1D}} = A/[A/\kappa + R_{\text{th}}(A/a - 1)], \quad (3)$$

reducing to

$$\kappa_{\text{av}}^{\text{1D}} = 1/(1/\kappa + R_{\text{th}}/a) \quad (4)$$

in the limit of $A \gg a$, which is well satisfied in the case investigated here. This simple relation can be used to relate our microscopic thermal data to overall lateral conductivity provided the average grain size is known. As the average grain size of our sample is 40 μm and the average thermal conductivity inside the grains is $\kappa = 2000$ W/mK, Eq. (4) yields a one-dimensional thermal conductivity $\kappa_{\text{av}}^{\text{1D}} = 1600$ W/mK confirmed by measurements of the manufacturer of the diamond sample.

In the following we use our microscopic data and Eq. (4) to describe measurements of CVD diamond presented in literature only by the knowledge of the average grain size. Such information, i.e., lateral conductivity as a function of grain size, has been provided by Graebner *et al.* for a set of samples grown under conditions very similar to that of our sample [14]. Therefore, it is justified to combine our microscopic thermal data with their macroscopic conductivity measurements and plug both into the one-dimensional heat flow model described above. From the published data on the thickness dependent grain size of these samples we calculate a mean grain size by taking the average from the grain size given for the thinnest diamond film (2.5 μm) and the grain size at the sample surface for a specific thickness. Surface grain size and averages used in our calculation together with the measured thermal conductivities and those predicted by our model, are given in Table I. Using a thermal conductivity of 2000 W/mK inside the grains and a thermal resistance of 2.4×10^{-9} m² K/W yields a reasonably good agreement between measured data and our predictions, as can be seen in Fig. 3. Of course, the rough model neglecting the details of the diamond microstructure like a grain size varying over the film thickness cannot precisely reproduce the functional relationship between average grain size and lateral conductivity. However, it well

TABLE I. Compilation of data used for applying the one-dimensional heat flow model [Eq. (4)] to grain size dependent average thermal conductivity measurements. The mean bulk grain size is calculated from the data for film thickness and surface grain size given in Ref. [14] where also one-dimensional thermal conductivity data for the respective films have been reported. The predicted values for the average in-plane thermal conductivity were calculated assuming a thermal conductivity of 2000 W/mK inside the grains and a thermal resistance of 2.4×10^{-9} m² K/W at grain boundaries.

Measured film thickness (μm)	Measured surf. grain size (μm)	Calc. mean bulk grain size a (μm)	Measured conductivity $\kappa_{\text{av}}^{\text{1D}}$ (W/mK)	Calculated conductivity $\kappa_{\text{av}}^{\text{1D}}$ (W/mK)
27.1	2.5 ± 0.5	2.5 ± 0.5	720 ± 36	685
69.2	6 ± 1.2	4.3 ± 0.8	880 ± 44	945
112	10 ± 2.0	6.3 ± 1.6	960 ± 48	1135
185	15.6 ± 3.1	9.1 ± 2.5	1360 ± 68	1309
355	23 ± 4.6	11.8 ± 3.8	1720 ± 86	1422

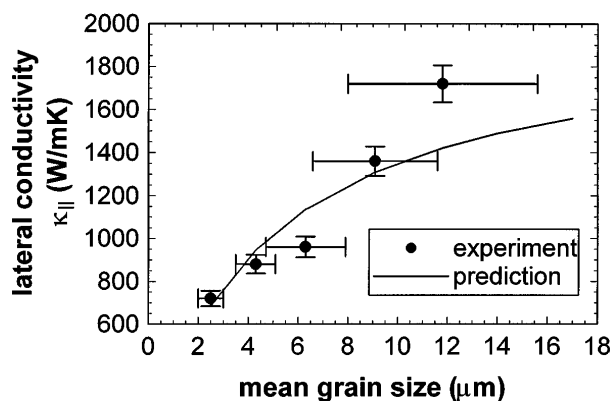


FIG. 3. Comparison of grain size dependent macroscopic lateral thermal conductivity data with predictions from a one-dimensional heat model [Eq. (4)]. Thermal data used as an input for the heat flow model are given in Table I and its caption.

fits the conductivity observed for the smallest grain size and predicts the right trend for increasing grain size. The fact that measured conductivities rise faster with grain size than predicted may be attributed to a variation in the quality of grain boundaries with film thickness. While a significant fraction of nondiamond material accumulated at grain boundaries is expected in the initial stages of nucleation and film growth, the thermal response of thicker samples will certainly be dominated by heat flow across higher quality grain boundaries.

In conclusion, we demonstrated for the first time the direct quantitative determination of thermal resistances at single thermal barriers located at grain boundaries in CVD diamond with μm resolution. Using a simple one-dimensional model of heat flow in the polycrystalline material, we calculated the effect of thermal barriers and grain size on the overall thermal conductivity. Applying the model to measured thermal parameters of CVD diamond films published by other authors we are able to predict experimental results of macroscopic thermal measurements only by the knowledge of the average grain size and microscopic thermal data.

Continued support of this work by E. Matthias is gratefully acknowledged. This work was funded by the Euro-

pean Community under Contract No. BRE2-0154 and by the Deutsche Forschungsgemeinschaft, Sonderforschungsbereich 337.

*Present address: Physikalisch-Technische Bundesanstalt, Abbestraße 2-12, 10587 Berlin, Germany.

Electronic address: dr.j.hartmann@ptb.de

†Corresponding author.

Electronic address: reichling@matth1.physik.fu-berlin.de

- [1] M. N. Yoder, in *Diamond Films and Coatings*, edited by R. F. Davies (Noyes Publications, Park Ridge, 1992), p. 1.
- [2] B. Fliegl, R. Kuhnert, H. Schwarzbauer, and F. Koch, *Diamond Relat. Mater.* **3**, 658 (1994).
- [3] J. A. Herb, III-Vs Rev. **4**, 41 (1991).
- [4] E. F. Borchert and G. Lu, in *Proceedings of the 6th International SAMPE Electronics Conference on Critical Materials and Processes in a Changing World, Covina, California, 1992*, edited by A. B. Goldberg, C. A. Harper, M. S. Schroeder, and A. M. Ibrahim (Society for the Advancement of Material and Process Engineering, Baltimore, 1992), p. 371.
- [5] J. E. Graebner, S. Jin, G. W. Kammlott, J. A. Herb, and C. F. Gardinier, *Nature (London)* **359**, 401 (1991).
- [6] J. E. Graebner, S. Jin, G. W. Kammlott, B. Bacon, L. Seibles, and W. Bannholzer, *J. Appl. Phys.* **71**, 5353 (1992).
- [7] J. E. Graebner, *Diamond Films Technol.* **3**, 77 (1993).
- [8] K. Plamann, D. Fournier, B. C. Forget, and A. C. Boccara, *Diamond Relat. Mater.* **5**, 699 (1996).
- [9] J. Hartmann, P. Voigt, and M. Reichling, *J. Appl. Phys.* **81**, 2966 (1997).
- [10] J. E. Graebner, M. E. Reiss, L. Seibles, T. M. Hartnett, R. P. Miller, and C. J. Robinson, *Phys. Rev. B* **50**, 3702 (1994).
- [11] G. Meyer-Berg, R. Osiander, P. Korpium, P. Kakoschke, and H. Joswig, *Photoacoustic and Photothermal Phenomena III*, in Springer Series in Optical Science Vol. 69, edited by D. Bicanic (Springer-Verlag, Berlin, 1992), p. 711.
- [12] H. S. Carslaw and J. C. Jaeger, *Conduction of Heat in Solids* (Oxford University Press, New York, 1959).
- [13] F. Lepoutre, *J. Phys. III (France)* **3**, 1531 (1993).
- [14] J. E. Graebner, S. Jin, G. W. Kammlott, J. A. Herb, and C. F. Gardinier, *Appl. Phys. Lett.* **60**, 1576 (1992).